

**All-optical transistor using a photonic-crystal cavity with an active Raman gain medium**

V. G. Arkhipkin\* and S. A. Myslivets

*L. V. Kirensky Institute of Physics, Siberian Branch of the Russian Academy of Sciences, 660036 Krasnoyarsk, Russian Federation*

(Received 24 May 2013; published 27 September 2013)

We propose a design of an all-optical transistor based on a one-dimensional photonic-crystal cavity doped with a four-level N-type active Raman gain medium. The calculated results show that in a photonic-crystal cavity of this kind transmission and reflection of the probe (Raman) beam are strongly dependent on the optical switching power. Transmission and reflection of the probe beam can be greatly amplified or attenuated. Therefore the optical switching field can serve as a gate field of the transistor to effectively control propagation of the weak probe field. It is shown that the group velocity of the probe pulse can be controlled in the range from subluminal (slow light) to superluminal (fast light).

DOI: [10.1103/PhysRevA.88.033847](https://doi.org/10.1103/PhysRevA.88.033847)

PACS number(s): 42.50.Gy, 42.55.Sa, 42.65.Dr, 42.70.Qs

**I. INTRODUCTION**

All-optical switching (AOS) and transistors where one light beam controls another light beam have been the subject of many recent studies (see, for example, [1–12]). They find many practical applications in optical communications, quantum information processing, and so on. For optical switches to operate efficiently it is necessary to have optical systems capable of producing large optical nonlinearities while having minimal linear absorption loss. Taking advantage of electromagnetically induced transparency (EIT) [13], where linear susceptibility vanishes while nonlinearity is greatly enhanced, absorptive [2] and dispersive [3] AOS can be realized at low light levels in an N-type atomic system. Absorptive AOS was experimentally demonstrated in hot atomic vapor [7] and cold atoms [4–6] in free space. A giant Kerr nonlinearity (cross-phase modulation) [3] was also used for AOS in an N-type atomic system [14,15]. Recently, an experimental demonstration of AOS has been reported using an optical ring cavity with three- and four-level atoms under EIT conditions [16–18]. A variety of other types of AOS has been realized based on enhanced Kerr nonlinearity [8], optical bistability [10], an electromagnetically induced absorption grating [11], and phase-controlled interference [12]. Recently all-optical microdisk switches and transistors have been proposed using EIT [19,20]. We note that most of the optical switching schemes are based on a control absorption or refractive index using different nonlinear optical effects.

Photonic-crystal (PC) structures combined with EIT offer new tools to control light by light [21–29]. In such structures, the nonlinear interaction becomes greatly amplified by a unique confinement of light and slow group velocity, and it can be realized at low intensities. In Ref. [25] an optical switch based on a PC cavity with giant Kerr nonlinearity [3] was proposed that can operate at low energy levels. An efficient absorptive AOS was demonstrated in [28] using slow light within a hollow PC fiber with cold atoms.

An alternative to the EIT schemes is a scheme with Raman gain in three- and four-level quantum systems [30–34]. Unlike the EIT-based scheme, which is inherently absorptive, the central idea of the Raman gain scheme is that the probe field

operates in a stimulated Raman emission mode, and hence attenuation of the probe field can be completely eliminated and both subluminal (slow light) and superluminal (fast light) propagation of optical waves can be realized [30–33]. Recently a fast Kerr phase gate using the Raman gain method has been experimentally demonstrated where the probe wave travels “superluminally” [35]. In the papers [36,37], we have theoretically demonstrated how one could use a three-level Raman gain medium together with a PC cavity to create an AOS where the pump field controls the probe (Raman) beam.

Here we present an approach to create an AOS based on a PC with a defect containing a four-level active Raman gain (ARG) medium as shown schematically in Fig. 1, where the Raman gain process can be coherently controlled by additional laser radiation (a switching field). Propagation of a weak (Raman) probe wave in a linear medium controlled by two coherent fields will be considered. We will show that the probe wave in such a PC cavity can be efficiently controlled by switching the laser field. The proposed scheme enables narrow resonances in transmission and reflection spectra of a PC to be obtained. The transmission and reflection coefficients of the probe light can be increased (beyond unity simultaneously) or decreased (to near zero) by varying the intensity of the switching field. Our study of propagation of the probe pulse in such a structure proves that the proposed device can operate as an all-optical transistor. We also show that the group velocity of the probe pulse in the proposed scheme can be controlled in the range from subluminal to superluminal.

The paper is organized as follows. In Sec. II we discuss the nonlinear Raman susceptibility of a four-level N-type medium in the presence of an additional switching field. In Sec. III we present the results of simulation of the spectral properties of a one-dimensional photonic crystal with a defect filled with an ARG medium. Section IV concludes the paper.

**II. THEORETICAL MODEL**

Consider a one-dimensional PC having the structure  $(HL)^p HDH(LH)^p$ . Such a structure is also called a photonic-crystal cavity [38]. Here H and L refer to different dielectric layers with a high (H) and a low (L) refractive index  $n_H$  and  $n_L$ , and the thicknesses  $t_H$  and  $t_L$ , respectively; D is the defect layer with the refractive index  $n_D$  and the thickness  $t_D$ ,  $t = t_H + t_L$  is the period of the structure;  $p$  is the number

\*avg@iph.krasn.ru

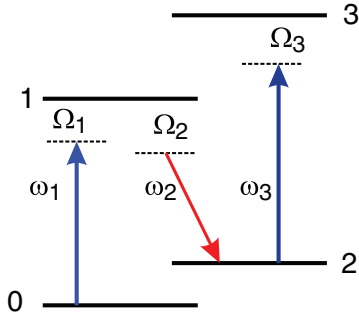


FIG. 1. (Color online) N-type four-level atomic system and coupling scheme.

of periods. The defect is filled with a Raman gain medium, which we will simulate by immobile four-level atoms with the energy levels as shown in Fig. 1 (N-type structure). We will assume that the atoms do not interact with each other. Only the lower ground state  $|0\rangle$  is initially populated, the  $|2\rangle$  state is metastable. Transitions  $|0\rangle\text{-}|1\rangle$ ,  $|1\rangle\text{-}|2\rangle$ , and  $|2\rangle\text{-}|3\rangle$  are allowed but the  $|0\rangle\text{-}|2\rangle$  transition is dipole forbidden (the Raman transition). Three plane monochromatic waves  $\varepsilon_j(z,t) = E_j \exp[-i(\omega_j t - k_j z)]$  are normally incident on the PC and propagate along the  $z$  axis ( $z = 0$  corresponds to the boundary of the first layer). Subscripts  $j = 1, 2, 3$  refer to the pump, probe, and switching fields, respectively;  $E_j$  is the wave amplitude, and  $\omega_j$  and  $k_j$  are the frequency and the wave number. Level  $|1\rangle$  is coupled with the two lower levels  $|0\rangle$  and  $|2\rangle$  via the pump field  $\varepsilon_1$  with frequency  $\omega_1$  and the probe field  $\varepsilon_2$  with frequency  $\omega_2$ . The frequency difference  $\omega_1 - \omega_2$  is close to the frequency of the Raman transition  $\omega_{20}$ . Applying a third field  $\varepsilon_3$  with frequency  $\omega_3$  that interacts with the  $|2\rangle\text{-}|3\rangle$  transition allows the Raman gain of the probe wave to be coherently controlled as well as inducing a cross-Kerr nonlinearity which can affect the refractive index and hence the group velocity of the probe [33]. We will assume the probe field intensity to be much lower than the intensity of the other two fields. Without a switching field, the probe light experiences Raman gain [39]. The intensity of the pump is chosen so as not to exceed the stimulated Raman scattering threshold while being sufficiently strong to ensure a noticeable enhancement of the probe wave. The pump field detuning from resonance is chosen such that single-photon absorption can be neglected.

The Raman gain coefficient (negative absorption) and the refractive index for the probe field are determined by the imaginary and real parts of the macroscopic nonlinear susceptibility. The latter can be found from the matrix density equations by solving them exactly in the switching field  $\chi(\omega_2)$ , to the second order in the pump field and the first order in the probe field. The susceptibility  $\chi(\omega_2)$  for the probe wave can then be written as [33]

$$\chi(\omega_2) = -i \frac{\beta |G_1|^2 (\Delta_{31} \Delta_{30} - |G_3|^2)}{\Delta_{10} [\Delta_{20} \Delta_{30} + |G_3|^2] [\Delta_{12}^* \Delta_{31} + |G_3|^2]}, \quad (1)$$

where  $2G_{1,3} = d_{01,23} E_{1,3} / \hbar$  are the Rabi frequencies of the pump and switching field,  $\beta = |d_{12}|^2 N / 2\hbar$ ,  $\Delta_{10} = \gamma_{10} + i\Omega_1$ ,  $\Delta_{20} = \gamma_{20} + i(\Omega_1 - \Omega_2) = \gamma_{20} + i\Omega_{20}$ ,  $\Delta_{30} = \gamma_{30} + i(\Omega_1 - \Omega_2 + \Omega_3) = \gamma_{30} + i\Omega_{30}$ ,  $\Delta_{31} = \gamma_{31} + i(\Omega_3 - \Omega_2) = \gamma_{31} + i\Omega_{31}$ , and  $\Omega_j = \omega_j - \omega_{mn}$  are the frequency

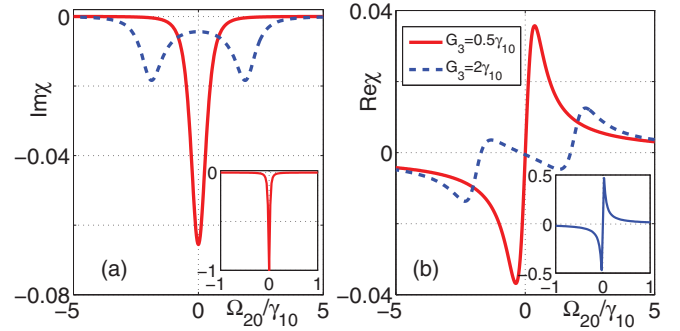


FIG. 2. (Color online) Normalized (a)  $\text{Im } \chi(\omega_2)$  and (b)  $\text{Re } \chi(\omega_2)$  vs detuning from the Raman resonance  $\Omega_{20} = \Omega_1 - \Omega_2$  ( $\Omega_2$  changes) for various Rabi frequencies  $G_3$ .  $G_1 = 5\gamma_{10}$ ,  $\Omega_{30} = 0$ . Insets: The same dependences for Raman susceptibility ( $G_3 = 0$ ).

detunings, and  $\Omega_{20} = \omega_1 - \omega_2 - \omega_{20}$ ,  $\Omega_{30} = \omega_1 - \omega_2 + \omega_2 - \omega_{30}$ ,  $\Omega_{31} = \omega_3 - \omega_2 - \omega_{31}$ ,  $\omega_{mn}$ , and  $\gamma_{mn}$  are the frequencies and half-widths of the respective transitions. Expression (1) was obtained assuming  $|\Omega_{1,2}| \gg \gamma_{10}, \gamma_{12}, G_1$ , and the ground-state population to be  $\rho_0 \approx 1$ .

When the switching field is weak ( $G_3 \ll |\Delta_{30}|$ ), the susceptibility (1) can be expressed as

$$\chi(\omega_2) = -i\beta \frac{|G_1|^2}{\Omega_1 \Omega_2 \Delta_{20}} + i\beta \frac{|G_1|^2 |G_3|^2}{\Omega_1 \Omega_2 \Delta_{20}^2 \Delta_{30}} = \chi_1 + \chi_2. \quad (2)$$

The first term in (2) is a standard Raman susceptibility with a normal dispersion in the vicinity of resonance [39] (see the curves in the insets in Fig. 2). The second term in (2), associated with the effect of the switching, results in modification of the Raman susceptibility.

The imaginary parts  $\chi_1$  and  $\chi_2$  have opposite signs in the vicinity of the Raman resonance  $|\Omega_{20}| < \gamma_{20}$  (destructive interference). This means that by applying a third field we induce nonlinear absorption of the probe field, which decreases the Raman gain [the solid curve in Fig. 2(a)]. It can be shown that for detunings from Raman resonance such that  $|\Omega_{20}| > \gamma_{20}$ , the imaginary part  $\text{Im } \chi_2$  has the same sign as  $\text{Im } \chi_1$  as long as the switching field intensity is below a certain value. This suggests that in this case the application of a third field results in an increased Raman gain (constructive interference).

When  $G_3 > \gamma_{30}$  there appears a dip in the gain spectrum [Fig. 2(a), dashed line], i.e., the gain peak splits into a doublet and dispersion of the refractive index may change from normal to anomalous. This is due to splitting of the  $|2\rangle$  level under the applied switching field. When dispersion is normal, the group velocity can be much slower than the light velocity in vacuum [30,37], whereas in the region of anomalous dispersion the probe pulse can travel at a group velocity exceeding the velocity of light—a superluminal effect.

In a steady-state approximation, any individual field  $E_i$  ( $i = 1, 2, 3$ ) in the  $j$ th layer ( $j$  corresponds to the layers H, L, and D) can be treated as a superposition of the forward (incident) and backward (reflected) waves:

$$E_{i,j} = A_{i,j}(z) \exp[iq_{i,j}(z - z_j)] + B_{i,j}(z) \exp[-iq_{i,j}(z - z_j)],$$

where  $A_{i,j}$  and  $B_{i,j}$  are the amplitudes of the forward and backward waves, respectively,  $q_{i,j} = k_i n_{ij}$ ,  $k_i = 2\pi/\lambda_i$ , and

$n_{ij}$  is the refractive index for the  $i$ th wave in the  $j$ th layer. The amplitudes  $A_{i,j}$  and  $B_{i,j}$  can be found from the appropriate wave equations by applying the recurrence-relations technique [23,40]. For this purpose, we divide all the photonic-crystal layers into a sufficiently large number  $K$  of sublayers such that the field can be assumed constant within each sublayer numbered  $m$ . By using the continuity conditions for electric and magnetic components of the fields at the interface of sublayers numbers  $m$  and  $m+1$ , we obtain a system of equations connecting the field amplitudes in adjacent sublayers (hereafter the subscript  $i$  is omitted):

$$\begin{aligned} A_m + B_m &= g_{m+1}^{-1} A_{m+1} + g_{m+1} B_{m+1}, \\ q_m(A_m - B_m) &= q_{m+1}(g_{m+1}^{-1} A_{m+1} - g_{m+1} B_{m+1}), \end{aligned} \quad (3)$$

where  $g_m = \exp(iq_m t_m)$ ,  $m = 1, 2, \dots, K+1$ ,  $t_m = z_{m+1} - z_m$  are the thicknesses of the sublayers, and the thickness of the last sublayer is  $t_{K+1} \equiv 0$ . The functions  $g_m$  take into account variations in the phases of the waves and their decay or amplification in the  $m$ th sublayer.

By introducing the amplitude reflection coefficients  $R_m = B_m/A_m$ , we can obtain a recurrent relation from Eq. (3), which connects the coefficients  $R_m$  and  $R_{m+1}$  in the adjacent sublayers:

$$R_m = \frac{r_m + g_{m+1}^2 R_{m+1}}{1 + r_m g_{m+1}^2 R_{m+1}}. \quad (4)$$

Here,  $r_m = (q_m - q_{m+1})/(q_m + q_{m+1})$ . By using relation (4), we find all  $R_m$ , starting from the right boundary of the photonic crystal, taking into account the boundary condition  $R_{K+1} = 0$ , and express  $A_{m+1}$  in terms of  $A_m$  in an arbitrary sublayer  $m$ :

$$A_{m+1} = A_m \frac{1 + R_m}{g_{m+1}^{-1} + g_{m+1} R_{m+1}}. \quad (5)$$

Using relation (5), we determine all  $A_m$ , starting from the left boundary of the photonic crystal. Then, we calculate the amplitude of the backward wave  $B_m = A_m R_m$ . The transmission spectra of the probe field are determined as

$$T = \left| \frac{A_{2L}}{A_{20}} \right|^2, \quad (6)$$

where  $A_{20}$  and  $A_{2L}$  are the input and output amplitudes of the probe wave.

### III. RESULTS AND DISCUSSION

Using the model specified in the previous section, we have calculated the transmission spectra of the probe field. Also propagation of the probe pulse has been considered for various Rabi frequencies of the switching field. For numerical simulation, we used sodium atomic parameters as the Raman medium. Wavelengths of the probe, pumping, and switching fields were chosen close to the  $D_1$  line and  $\omega_{20}$  was chosen to be 1.8 GHz. The PC had the following parameters:  $p = 5$ ,  $n_H d_H = n_L d_L = \lambda/4$ ,  $d_D = \lambda/2$ ,  $n_H = 2.35$ , and  $n_L = 1.45$ . The rest of the parameters were as follows:  $\gamma_{10} = \gamma_{30} = 2\pi \times 5.7 \times 10^6 \text{ s}^{-1}$ ,  $\Omega_1 = 30\gamma_{10}$ ,  $\gamma_{20} = 2\pi \times 10^5 \text{ s}^{-1}$ , and  $N \simeq 10^{12} \text{ cm}^{-3}$ . The refractive index for the probe field in the defect layer is calculated by the formula  $n_D = 1 + 2\pi N \text{Re}\{\chi(\omega_2)\}$  [41].

The PC parameters have been chosen such that the defect mode (DM) is located in the center of the gap and its spectral width is broad enough for all three waves to fall within this transmission band. The DM resonance frequency coincides with that of the probe wave under Raman resonance  $\Omega_{20} = 0$ . Light fields are localized in the defect: the maximum intensity occurs in the center of the defect, decreasing virtually down to zero towards the edges of the defect. The intensities of the pump and switching fields are, respectively, about 700 times and 200 times higher in the center of the defect than at the entrance into the PC.

Since we assume that in a defect layer  $G_{1,3} \gg G_2$ , simulation of the transmission coefficient for the probe field was performed in the undepleted-pump approximation. The complex refractive index was calculated using the susceptibility (1). The fields are distributed inhomogeneously across the defect, and therefore the gain factor and the refractive index in the defect are functions of the  $z$  coordinate. The Rabi frequency in the defect  $G(z)$  is related to the Rabi frequency  $g$  at the entrance into the PC as follows:  $G(z) = gF(z)$ , where  $F(z) = |E(z)|/|E_{in}|$  is the amplification factor of the field amplitude in the defect,  $E(z)$  is the spatially dependent field strength in the defect, and  $E_{in}$  is the strength of the incident field.

The PC transmission spectra are shown in Fig. 3 (see the main panel and right inset) for selected Rabi frequencies of the switching field  $g_3$ . Initially, we chose  $g_1 = 0.2\gamma_{10}$  so that the PC transmission was close to zero under Raman resonance, which corresponds to the right-hand branch of the transmission coefficient plotted in the left inset in Fig. 3 [36,37]. In this case there is a dip in the center of the transmission spectrum (a solid curve). The transmission increases when a third field is applied (a dashed curve). Starting from a certain value  $g_3$ , the dip in transmission turns into an enhancement peak (a dash-dotted curve and a solid curve in the right inset). By means of a switching field we can thus control the transmission coefficient of a PC, amplifying or virtually completely eliminating the output probe field. The same applies to the case of

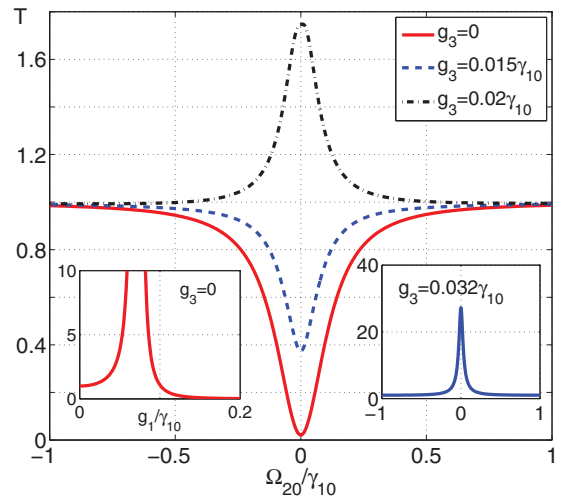


FIG. 3. (Color online) Transmission spectra of the PC for the probe field at various  $g_3$ .  $g_1 = 0.2\gamma_{10}$ . Left inset: transmission coefficient for the probe field vs  $g_1$  under  $\Omega_{20} = 0$ .

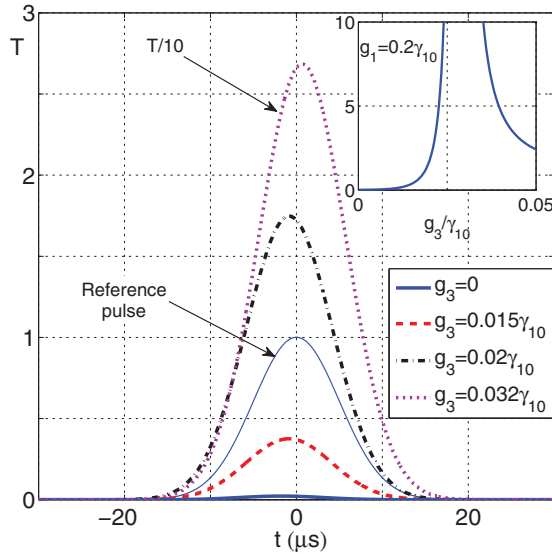


FIG. 4. (Color online) Time dependence of the probe pulse transmitted through a PC cavity with ARG medium for various  $g_3$ . The thin solid curve illustrates the reference pulse (empty PC cavity and  $g_3 = 0$ ). The length of the incident Gaussian probe pulse is  $20 \mu\text{s}$ .  $g_1 = 0.2\gamma_{10}$ . Right inset: the transmittance of the probe field vs  $g_3$ . Left inset: the spectral dependencies of the phase of the transmitted probe wave.

reflection. Consider now propagation of a probe pulse. We assume the pump and the switching fields to be continuous monochromatic waves. The spectrum of the transmitted probe pulse can be written as  $E_{2t}(\omega) = T(\omega)E_{2i}(\omega)$ , where  $T(\omega)$  is the transmission coefficient, and  $E_{2i}(\omega)$  is the spectrum of the incident probe pulse. Applying a reverse Fourier transform, the intensity of the transmitted probe pulse can be written as [29,42]

$$I_{2t}(t) \propto \left| \frac{1}{\sqrt{2\pi}} \int_{-\infty}^{\infty} T(\omega) E_{2i}(\omega) \exp(-i\omega t) d\omega \right|^2. \quad (7)$$

In terms of this approach, the duration of the probe pulse  $\tau_2$  must satisfy the requirement that  $\tau_2 \gg |\Delta_{20}|^{-1}$  [32].

Figure 4 illustrates a transmitted Gaussian probe pulse for various Rabi frequencies of the incident switching field  $g_3$ . The pump field intensity was chosen so as to virtually stop transmission of the probe pulse through the PC (thick solid curve). The thin solid curve refers to the transmitted probe pulse when there is no Raman medium in the defect—the reference pulse. As seen from the figure, in a PC with Raman nonlinearity the transmission can be controlled from enhancing to eliminating the latter by varying the switching field intensity. Thus, subject to a proper choice of parameters, *the system can operate as an all-optical transistor*. The intensity required for these effects to be observed depends on a number of factors (frequency detunings, Raman resonance width, quality factor of defect modes) and can be anything in the range from several  $\mu\text{W}/\text{cm}^2$  (for the switching field) to hundreds of  $\mu\text{W}/\text{cm}^2$  (for the pump). These intensities, as indicated by the estimates, correspond to 1–100 photons in a  $20 \mu\text{s}$  pulse per area  $\lambda^2$ . Implementation of a single-photon level switch does not require high- $Q$  resonances and the

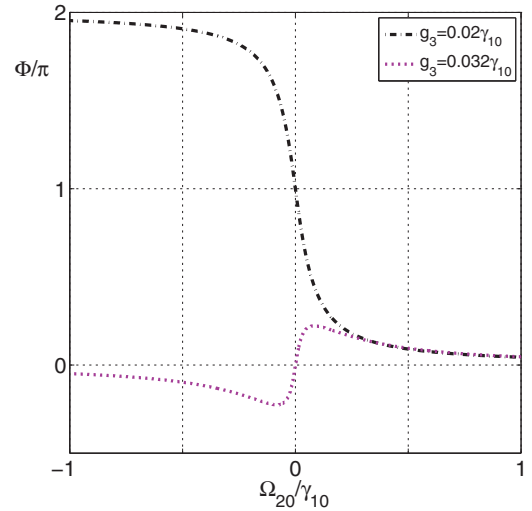


FIG. 5. (Color online) Spectral dependencies of the phase of transmitted probe wave for different Rabi frequencies of a switching field.

bandwidth of operation will be limited to the lifetime of coherence of the Raman transition as in [35].

Furthermore, from Fig. 4 it follows that depending on the switching field intensity the transmitted probe pulse may either lag behind (the dotted curve) the reference pulse or lead the latter (the dashed and dash-dotted curves). In the first case we say that the group velocity of the pulse is lower than the speed of light in vacuum (subluminal propagation). In the second case the group velocity is larger than the speed of light in vacuum (superluminal propagation) [43].

The inset in Fig. 4 is a plot of the transmission coefficient  $T$  of the probe field versus the Rabi frequency of the switching field  $g_3$  for  $g_1 = 0.2\gamma_{10}$ . The transmission coefficient grows when the pump intensity increases, yet remaining below a certain threshold value. Beyond this critical value, the transmission decreases with growing intensity (the peak in transmission turns into a dip). When  $g_3$  corresponds to the left-hand branch of the curve in the right inset, i.e., below the

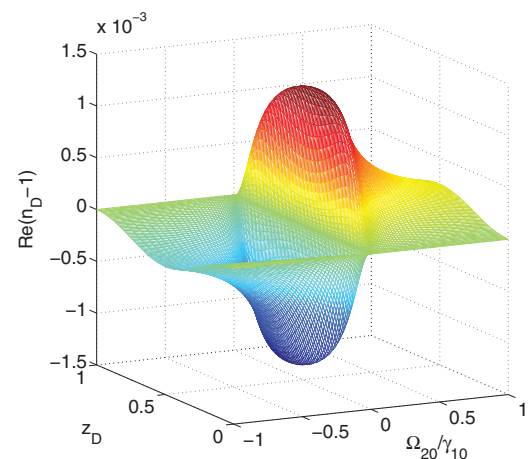


FIG. 6. (Color online) . The dependence of  $\text{Re}(n_D - 1)$  vs the detuning  $\Omega_{20}$  and the normalized coordinate  $z_D$  in the defect layer for  $g_3 = 0.02\gamma_{10}$  and  $g_1 = 0.2\gamma_{10}$ .

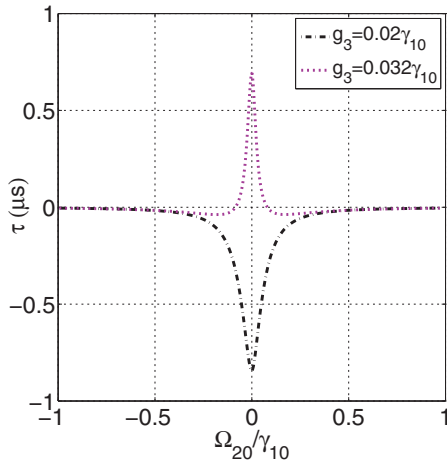


FIG. 7. (Color online) The group delay  $\tau$  as function of detuning from the Raman resonance  $\Omega_{20}$  for different Rabi frequencies  $g_3$ .

threshold, we deal with superluminal propagation, and with  $g_3$  corresponding to the right-hand branch (beyond the threshold) we observe subluminal propagation.

The time delay (group delay) of the pulse through the whole structure is defined as  $\tau = t_0(c/v_g - 1)$ , where  $t_0$  is the time over the same vacuum distance,  $v_g = c/n_g$  is the group velocity, and  $n_g$  is the group index [43,44]. The group velocity of the pulse depends on the behavior of dispersion of the refractive index (normal or anomalous); therefore the results obtained can be qualitatively explained in terms of the effective refractive index  $n_{\text{eff}}(\omega) = n(\omega) + ik(\omega)$  for the PC, which is related to the amplitude coefficient of the transmission  $t_a = \sqrt{T} \exp[i\Phi(\omega)]$ , where  $\Phi(\omega)$  is the phase of the probe wave passed through the PC [45,46]. The real part of  $n_{\text{eff}}(\omega)$  is

$$n(\omega) = c\Phi(\omega)/\omega L,$$

and its imaginary part is

$$k(\omega) = -c \ln T(\omega)/2\omega L.$$

Obviously,  $n(\omega)$  or  $\Phi(\omega)$  describes the dispersion properties of the PC structure, while  $k(\omega)$  is responsible for enhancement or dissipation in such a structure. For a PC with an empty defect, dispersion in the region of DM is normal and hence the group velocity will be lower than the speed of light in vacuum [44].

Figure 5 shows spectral dependences of the phase  $\Phi(\omega)$  of the transmitted probe wave for two values of  $g_3$ : below (the dash-dotted curve,  $g_3 = 0.02\gamma_{10}$ ) and above (the dotted curve,  $g_3 = 0.032\gamma_{10}$ ) the threshold. Dispersion in the first case is anomalous; therefore we deal with superluminal propagation, i.e., the transmitted probe pulse leads the reference pulse, whereas dispersion in the second case is normal, which results in subluminal propagation of the probe pulse as illustrated in Fig. 4. It should be noted that the dispersion of medium in the defect remains normal under the above parameters as can

be seen from Fig. 6. We emphasize that the mechanism of attaining anomalous dispersion in the given case is essentially different from those reported in [33,34] and is associated with dispersion of the PC cavity (the structural dispersion) rather than with dispersion of the Raman medium (the material dispersion).

The group delay for the transmitted pulses can be calculated as [47]

$$\tau = \partial\Phi_t/\partial\omega|_{\omega=\omega_0},$$

where  $\omega_0$  is the pulse carrier frequency. Figure 7 shows the group delay  $\tau$  as a function of the detuning from the Raman resonance  $\Omega_{20}$  for different Rabi frequencies  $g_3$ . At the Raman resonance the maximal group delay are  $\tau(g_3 = 0.02\gamma_{10}) = -0.84 \mu\text{s}$ , and  $\tau(g_3 = 0.032\gamma_{10}) = 0.68 \mu\text{s}$ . One can see that these group delays at the Raman resonance correspond to those shown in Fig. 4.

#### IV. CONCLUSIONS

We have presented a design of an all-optical switch based on a PC with a defect containing a four-level active Raman gain medium. Unlike the widely used weakly driven EIT-based schemes, which are absorptive, the scheme discussed herein is based on coherent manipulation of the Raman gain by applying a low-power switching field. The gain-assisted nature of the Raman process combined with the unique properties of the PC cavity creates a situation when the probe field can be enhanced in such a system (the transmission coefficient being greater than unity) or suppressed (the transmission coefficient being much smaller than unity). As a result, this device can operate as an all-optical transistor with a low switching laser power. The achievable values are sensitive to the relaxation parameters and switching field detuning. For certain parameter values the switching field power can be as low as single photons. The switch size can be considerably smaller than in a conventional cell. We also theoretically demonstrated the ability to control the dispersion of the photonic crystal structure from normal to anomalous. Thus in such systems one can control the group velocity of the probe pulse over the range from subluminal to superluminal. The occurrence of large positive and negative time delays is the result of the Bragg resonance coupled with the Raman resonance. Similar effects take place in reflection. The use of heterostructure semiconductors as nonlinear media with controlled Raman gain is of great interest. This opens up additional prospects for developing fast nonlinear switches and gates for information science.

#### ACKNOWLEDGMENTS

This work was supported in part by the RAS Grants No. 24.29, No. 24.31, and No. 3.9.5, by SB RAS Grants No. 43 and No. 101, and by the Ministry of Education and Science of the Russian Federation (State Contract No. 14.V37.21.0730).

- [1] H. M. Gibbs, *Optical Bistability: Controlling Light with Light* (Academic, New York, 1985).  
 [2] S. E. Harris and Y. Yamamoto, *Phys. Rev. Lett.* **81**, 3611 (1998).

- [3] H. Schmidt and A. Imamoglu, *Opt. Lett.* **21**, 1936 (1996).  
 [4] M. Yan, E. G. Rickey, and Y. Zhu, *Phys. Rev. A* **64**, 041801 (2001).

- [5] D. A. Braje, V. Balić, G. Y. Yin, and S. E. Harris, *Phys. Rev. A* **68**, 041801 (2003).
- [6] Y.-F. Chen, Z.-H. Tsai, Y.-C. Liu, and I. A. Yu, *Opt. Lett.* **30**, 3207 (2005).
- [7] W. Jiang, Q.-f. Chen, Y.-s. Zhang, and G.-C. Guo, *Phys. Rev. A* **73**, 053804 (2006).
- [8] H. Wang, D. Goorskey, and M. Xiao, *Phys. Rev. A* **65**, 051802 (2002).
- [9] H. Schmidt and R. J. Ram, *Appl. Phys. Lett.* **76**, 3173 (2000).
- [10] A. Brown, A. Joshi, and M. Xiao, *Appl. Phys. Lett.* **83**, 1301 (2003).
- [11] A. W. Brown and M. Xiao, *Opt. Lett.* **30**, 699 (2005).
- [12] H. Kang, G. Hernandez, J. Zhang, and Y. Zhu, *Phys. Rev. A* **73**, 011802 (2006).
- [13] M. Fleischhauer, A. Imamoglu, and J. P. Marangos, *Rev. Mod. Phys.* **77**, 633 (2005).
- [14] H. Kang and Y. Zhu, *Phys. Rev. Lett.* **91**, 093601 (2003).
- [15] H.-Y. Lo, Y.-C. Chen, P.-C. Su, H.-C. Chen, J.-X. Chen, Y.-C. Chen, I. A. Yu, and Y.-F. Chen, *Phys. Rev. A* **83**, 041804 (2011).
- [16] H. Wang, D. Goorskey, and M. Xiao, *Opt. Lett.* **27**, 1354 (2002).
- [17] X. Wei, J. Zhang, and Y. Zhu, *Phys. Rev. A* **82**, 033808 (2010).
- [18] J. Sheng, X. Yang, U. Khadka, and M. Xiao, *Opt. Express* **19**, 17059 (2011).
- [19] B. Clader, S. Hendrickson, R. Camacho, and B. Jacobs, *Opt. Express* **21**, 6169 (2013).
- [20] B. D. Clader and S. M. Hendrickson, *J. Opt. Soc. Am. B* **30**, 1329 (2013).
- [21] M. Soljacic and J. D. Joannopoulos, *Nat. Mater.* **3**, 211 (2004).
- [22] M. Soljacic, E. Lidorikis, L. V. Hau, and J. D. Joannopoulos, *Phys. Rev. E* **71**, 026602 (2005).
- [23] V. G. Arkhipkin and S. A. Myslivets, *Quantum Electron.* **39**, 157 (2009).
- [24] J. Tidström, C. W. Neff, and L. M. Andersson, *J. Opt.* **12**, 035105 (2010).
- [25] M. Soljacic, E. Lidorikis, J. D. Joannopoulos, and L. V. Hau, *Appl. Phys. Lett.* **86**, 171101 (2005).
- [26] P. S. Light, F. Benabid, G. J. Pearce, F. Couny, and D. M. Bird, *Appl. Phys. Lett.* **94**, 141103 (2009).
- [27] S. Ghosh, A. R. Bhagwat, C. K. Renshaw, S. Goh, A. L. Gaeta, and B. J. Kirby, *Phys. Rev. Lett.* **97**, 023603 (2006).
- [28] M. Bajcsy, S. Hofferberth, V. Balic, T. Peyronel, M. Hafezi, A. S. Zibrov, V. Vuletic, and M. D. Lukin, *Phys. Rev. Lett.* **102**, 203902 (2009).
- [29] V. G. Arkhipkin and S. A. Myslivets, *Phys. Rev. A* **86**, 063816 (2012).
- [30] M. G. Payne and L. Deng, *Phys. Rev. A* **64**, 031802 (2001).
- [31] K. J. Jiang, L. Deng, and M. G. Payne, *Phys. Rev. A* **74**, 041803 (2006).
- [32] K. J. Jiang, L. Deng, and M. G. Payne, *Phys. Rev. A* **76**, 033819 (2007).
- [33] G. S. Agarwal and S. Dasgupta, *Phys. Rev. A* **70**, 023802 (2004).
- [34] K. J. Jiang, L. Deng, E. W. Hagley, and M. G. Payne, *Phys. Rev. A* **77**, 045804 (2008).
- [35] R. B. Li, L. Deng, and E. W. Hagley, *Phys. Rev. Lett.* **110**, 113902 (2013).
- [36] V. G. Arkhipkin and S. A. Myslivets, *Phys. Rev. A* **80**, 061802 (2009).
- [37] V. G. Arkhipkin and S. A. Myslivets, *JETP* **111**, 898 (2011).
- [38] K. J. Vahala, *Nature (London)* **424**, 839 (2003).
- [39] S. A. Akhmanov and N. I. Koroteev, *Methods of Nonlinear Optics in Light Scattering Spectroscopy* (Nauka, Moscow, 1981) (in Russian).
- [40] A. V. Balakin, V. A. Bushuev, B. I. Mantsyzov, I. A. Ozheredov, E. V. Petrov, A. P. Shkurinov, P. Masselin, and G. Mouret, *Phys. Rev. E* **63**, 046609 (2001).
- [41] R. W. Boyd, *Nonlinear Optics* (Academic, London, 1992).
- [42] J. Zhang, G. Hernandez, and Y. Zhu, *J. Mod. Opt.* **56**, 1955 (2009).
- [43] P. W. Milonni, *Fast Light, Slow Light and Left-Handed Light* (Taylor & Francis, New York, 2005).
- [44] R. W. Boyd, *J. Opt. Soc. Am. B* **28**, A38 (2011).
- [45] N.-h. Liu, S.-Y. Zhu, H. Chen, and X. Wu, *Phys. Rev. E* **65**, 046607 (2002).
- [46] M. Centini, C. Sabilia, M. Scalora, G. D'Aguzzo, M. Bertolotti, M. J. Bloemer, C. M. Bowden, and I. Nefedov, *Phys. Rev. E* **60**, 4891 (1999).
- [47] V. S. C. M. Rao, S. Gupta, and G. S. Agarwal, *Opt. Lett.* **29**, 307 (2004).